AIP Journal of Applied Physics

Interactions between magnetic nanoparticles and model lipid bilayers—Fourier transformed infrared spectroscopy (FTIR) studies of the molecular basis of nanotoxicity

M. Kręcisz, J. D. Rybka, A. J. Strugała, B. Skalski, M. Figlerowicz, M. Kozak, and M. Giersig

Citation: Journal of Applied Physics **120**, 124701 (2016); doi: 10.1063/1.4962951
View online: http://dx.doi.org/10.1063/1.4962951
View Table of Contents: http://scitation.aip.org/content/aip/journal/jap/120/12?ver=pdfcov
Published by the AIP Publishing

Interactions between magnetic nanoparticles and model lipid bilayers—Fourier transformed infrared spectroscopy (FTIR) studies of the molecular basis of nanotoxicity

M. Kręcisz,[1] J. D. Rybka,[1] A. J. Strugała,[1,2] B. Skalski,[1] M. Figlerowicz,[2] M. Kozak,[3,a)] and M. Giersig[1,4]
[1]*Faculty of Chemistry, Adam Mickiewicz University, Umultowska 89B, 61-614 Poznan, Poland*
[2]*Institute of Bioorganic Chemistry, Polish Academy of Science, Z. Noskowskiego 12/14, 61-704 Poznan, Poland*
[3]*Faculty of Physics, Adam Mickiewicz University, Umultowska 85, 61-614 Poznan, Poland*
[4]*Institut für Experimentalphysik, Freie Universität Berlin, Arnimalle 14, 14195 Berlin, Germany*

(Received 3 April 2016; accepted 4 September 2016; published online 22 September 2016)

The toxicity of nanoparticles (nanotoxicity) is often associated with their interruption of biological membranes. The effect of polymer-coated magnetic nanoparticles (with different Fe_3O_4 core sizes and different polymeric coatings) on a model biological membrane system of vesicles formed by dimyristoylphosphatidylcholine (DMPC) was studied. Selected magnetic nanoparticles with core sizes ranging from 3 to 13 nm (in diameter) were characterised by transmission electron microscopy. Samples with 10% DMPC and different nanoparticle concentrations were studied by attenuated total reflectance—Fourier transform infrared spectroscopy to establish the influence of nanoparticles on the phase behaviour of model phospholipid systems. *Published by AIP Publishing.*
[http://dx.doi.org/10.1063/1.4962951]

I. INTRODUCTION

In recent years, nanoparticles have become increasingly useful materials that could be used in many fields. The most promising possibilities of nanoparticles are their use in biomedical applications.[1–6] Such potential applications include the use of magnetic nanoparticles (MNPs) in nuclear magnetic resonance (NMR) imaging (MRI),[7] cancer therapy (hyperthermia),[8] cancer diagnostics,[9] and gene therapy as well as components of drug-delivery systems.[10,11] Therefore, it is important to estimate the cytotoxicity of nanoparticles, which determines the potential medical applications of MNPs.[1–6] The toxicity of nanoparticles (nanotoxicity) is often associated with the possibility of their interruption of biological membranes.[3] Another problem concerns the loss of the protective shell by MNPs and the release of the magnetic core into the cell. Direct interactions of the magnetite core with cell components could lead to homeostatic disturbances that result in oxidative stress, destruction of the cell cytoskeleton, and genetic changes.[1,11]

Nanoparticles can strongly interact with phospholipid membranes by adsorption to their surface or by affecting their integrity through the endocytic processes leading to pore formation. Nanoparticles may also penetrate into cells through diffusion or ion channels.[1,3] In nanoparticles with a silver core, the interaction of nanoparticles with biological membranes depends strongly on the physicochemical properties of the interacting particles (size, shape, and charge of nanoparticles).[1,4–6] The key parameters determining the nature of interactions are the size[1,5] and the shape[12] of the particles.[1] Theoretical models have postulated that spherical nanoparticles in the size range of 20–30 nm should interact most strongly with membranes, whereas those with diameters below this range should be involved in weaker interactions.[13,14] A model developed to investigate the mechanism of clathrin-free entry of a virus into cells showed that an optimal radius for spherical particles corresponds to 27–30 nm and proved the size dependency of interaction between nanoparticles and membranes.[15] However, several studies[14] have confirmed that these interactions are different for small nanoparticles.[16] Larger nanoparticles penetrate into the hydrophobic space of a lipid bilayer and may interact with membranes by the formation of membrane pores.[4] Nanoparticles that are smaller or comparable in size to the thickness of the membrane can interact extensively with the membrane, greatly affecting membrane integrity.[1] Molecular dynamics simulations of the passive uptake of ligand-coated nanoparticles showed a strong shape dependency of this process.[17,18] Sphero-cylindrical particles are found to have higher efficiency of passive endocytosis than spheres. Moreover, particles with sharp edges undergo no endocytosis.[17] Also, orientation of the rod-like nanoparticles during cellular uptake was found to be crucial in complete wrapping.[19] Using theoretical analysis and molecular simulations of cellular uptake of elastic nanoparticles, it was shown that stiffer particles can achieve full wrapping more easily than softer particles, whereas softer particles experience smaller energy changes during wrapping.[20] Depending on the chemical nature of the coated nanoparticles, they may penetrate into the interior of the membrane bilayer (hydrophobic or non-polar nanoparticles) or cause the formation of pores or holes in the bilayer (hydrophilic or charged nanoparticles), even leading to complete interruption of the biological membrane.[1,4,18] As a result of electrostatic interactions,

a)Author to whom correspondence should be addressed. Electronic mail: mkozak@amu.edu.pl. Telephone: +48-61-8295266. Fax: +48-61-8295245.

small hydrophilic nanoparticles can draw phospholipid molecules from the lipid membrane and arrange them into hybrid micelles composed of a nanoparticle core and a lipid-bilayer shell.[4,22–24] Structural studies have shown that spherical nanoparticles typically interact with the membrane.[1,21,25]

The current study was conducted to determine the effect of polymer-coated magnetic nanoparticles (with different magnetic core sizes and covered with different polymeric coatings) on a model biological membrane system made of vesicles formed by dimyristoylphosphatidylcholine (DMPC).

To study the effect of nanoparticles on the structure of biological membranes, the membrane model was DMPC, which is one of the main components of biological membranes. Fully hydrated phospholipids in a suitable concentration can form lamellar structures, which are a reasonable model of biological membranes.[26,27] The model of the interactions of nanoparticles with such biostructures relies on some simplifications because in living cells, lipid membranes are composed of many components (such as different membrane proteins, including pores or receptors), which may facilitate the diffusion and transport of nanoparticles.

Phospholipid molecules consist of a hydrophilic head and hydrophobic tail chains. Lamellar phases in solution under the influence of temperature undergo structural changes. Phase transitions are possible because the molecules in the interior of phospholipid bilayers may assume different conformations of hydrophobic chains (trans and gauche). In more ordered phases formed by phospholipids, acyl chains prevail in the trans conformation, whereas gauche conformers dominate in less ordered phases.[28,29] For DMPC in an aqueous environment, four structural phases are observed between which phase transitions occur at certain temperatures.[30] Subgel phase L_c undergoes a transition into planar gel phase $L_{\beta'}$ (a so-called sub-transition) at a temperature of approximately 279–280 K. Then, the planar phase $L_{\beta'}$ is transformed to the reverse gel phase $P_{\beta'}$ (sub-transition) at 288 K. The most important structural transformation, involving a fundamental change in the conformation of the acyl chains from the trans to gauche conformation, occurs at the transition from the inverted gel phase $P_{\beta'}$ to the L_α liquid crystalline phase. This transition is referred to as the major phase transition and occurs at 297 K.[30–32]

To analyse the structural changes of biological membranes induced by magnetic nanoparticles, we decided to use attenuated total reflectance—Fourier transform infrared spectroscopy (ATR-FTIR) and electron transmission microscopy (TEM). ATR-FTIR is a useful and non-invasive method for the study of phospholipid structures in aqueous solutions.[33–35]

The analysis of symmetric and asymmetric vibrations (2.800–3.000 cm^{-1}) derived from the CH_2 and CH_3 groups of the acyl chains of phospholipids is extremely useful, providing information on conformational changes within the phospholipid bilayer. Shifts of absorption bands characteristic of the methyl and methylene groups of phospholipid hydrophobic chains observed in the appropriate temperature range can specify the phase transitions of phospholipids. In addition, a vibrational analysis of PO_2^- and carbonyl groups allows for the specification of the behaviour at the phospholipid bilayer surface.[28,29] FTIR has been used previously to study surface interactions of iron oxides with phospholipids[36,37] and cells.[38,39] However, this study is the first to analyse interactions between phospholipid membranes and spherical magnetite nanoparticles.

II. MATERIALS AND METHODS

A. Synthesis of nanoparticles

1. Iron oxide nanoparticles in organic solvent: 3, 10, 13 nm (in diameter)

Iron oxide nanoparticles (10 nm) were synthesised by thermal decomposition in an organic solvent according to Sun's method.[40] Liquid iron pentacarbonyl (0.4 ml, 3.04 mmol) was injected into a mixture of 20 ml of 1-octadecene and 1.92 ml of oleic acid (6.08 mmol) at 100 °C. The resulting solution was heated and refluxed for 1 h, and then the mixture was cooled to room temperature. The solution was treated by excess ethanol and separated by centrifugation. The resulting mixture was dispersed in chloroform. Nanoparticles with diameters of 3 and 13 nm were synthesised in a similar manner but with varying molar ratios of $Fe(CO)_5$ to oleic acid (1:1 and 1:3 molar ratios, respectively) and were refluxed for 2 h.

2. Polymer synthesis

a. Polymer A—Polyacrylic acid modified by polyallylamine hydrochloride. Polyacrylic acid (0.041 g) was dissolved in 10 ml of DMF (dimethylformamide), and 0.5 g of polyallylamine hydrochloride was added into the solution. The reaction mixture was stirred for 2 h, and then 0.0036 g of 1-ethyl-3-(3-dimethylaminopropyl)carbodiimide (EDC) was added. The solution was stirred at room temperature for the next 24 h. Finally, DMF was removed by reduced pressure, and the mixture was redispersed in 7 ml of water.

b. Polymer B—Polyacrylic acid modified by N-octyl amine. The modification process of polyacrylic acid (polymer B) was conducted according to the method of Insin.[41] Polyacrylic acid (1 g) was dissolved in 10 ml of DMF (dimethylformamide), and 0.72 g of N-octyl amine was added to the solution. The reaction mixture was stirred for 2 h, and then 1.06 g of 1-ethyl-3–(3-dimethylaminopropyl) carbodiimide (EDC) was added. In the next step of the reaction, the mixture was stirred at room temperature for 20 h. DMF was then removed under reduced pressure, and 2 ml of water with 1 g of tetramethylammonium hydroxide was added and stirred for 2 h. After stirring, 4 ml of 1.3 M hydrochloric acid was added to the mixture to re-precipitate mPAA, and the supernatant was removed. The final product, purified mPAA (polymer B), was then dissolved and kept in ethyl acetate.

3. Coating process

a. Coating process of iron oxide (3 nm) by polymer A. In chloroform, 8 mg of magnetic NPs (3 nm) was mixed with 3 ml of polymer A for 12 h. The chloroform content in the mixture was slowly reduced by low pressure, and water was added dropwise during sonication. Nanoparticles (in water solution) prepared in this manner are denoted as 3 A.

b. Coating process of iron oxide (3, 10, and 13 nm) by polymer B. A 1.5-ml volume of polymer B solution was mixed with 5 mg of iron oxide nanoparticles (3, 10, and 13 nm). Then, chloroform was removed under reduced pressure, and nanoparticles were dispersed in water. The samples prepared in this manner are denoted as 3B, 10B, and 13B.

4. Modification of MNPs with PEG

a. Modification of MNPs by O-(2-aminopropyl)-O′-(2-methoxyethyl)polypropylene ethylene glycol (PEG1). Samples 3A, 10B, and 13B (3 nm, 10 nm, 13 nm) of polymer-coated magnetic NPs in water were mixed with 0.003 g of EDC for 2 h. Then, 10 μl of O-(2-aminopropyl)-O′-(2-methoxyethyl)-polypropylene ethylene glycol (PEG1) was added. The mixture was stirred for 12 h.[42] Afterwards, the resulting solution was centrifuged three times to remove excess surfactants. Finally, the solution was redispersed into water. The samples prepared in this way are denoted as 3A1, 10B1, and 13B1.

b. Modification of MNPs by bis(3-aminopropyl) polyethylene glycol (PEG2). Sample 3B nanoparticles (3 nm NPs coated with polymer B) were modified with bis(3-aminopropyl) polyethylene glycol (PEG2) using the same procedure as for 3A1. The MNP samples prepared in this manner are denoted as 3B2.

c. Modification of MNPs by O,O′-bis(2-aminopropyl)polypropylene-(glycol-block-polyethylene)(glycol-block-polypropylene) glycol (PEG3). The same procedure as for previous samples was used for the modification of 3A samples (3 nm NPs coated with polymer A) with O,O′-bis(2-aminopropyl)-polypropylene glycol-block-polyethylene glycol-block-polypropylene glycol (PEG3). The samples modified in this manner are denoted as 3A3.

Finally, for FTIR studies, we selected the MNPs denoted as 3A1, 3A3, 3B2, 10B1, and 13B1.

B. Preparation of DMPC and DMPC/MNP nanosystems

DMPC (1,2-dimyristoyl-sn-glycero-3-phosphocholine) was purchased from Avanti Polar Lipids (Alabaster, Alabama, USA). Dry DMPC powder was dissolved in deuterium oxide (SIGMA). DMPC suspensions for FTIR studies were prepared by five cycles of alternating heating above the transition temperature and cooling for 30 min after each step according to previously published procedures.[26]

DMPC/MNPs systems for selected concentrations of nanoparticles (0.02, 0.04, and 0.05 mg/ml) were prepared by the direct addition of an appropriate amount of the nanoparticle solution to DMPC solutions (final concentration of 10%). Then, the mixtures were sonicated for 15 min at a temperature below the main phase transition.

Samples were denoted with phospholipid name, nanoparticle size, polymer type, and the number indicating the MNPs concentration, from the lowest, −0.02 mg/ml, labeled as 1; to the highest, 0.05 mg/ml, labeled as 3. For example, notification DMPC/13B1/2 means that the sample is a 10% solution of DMPC containing nanoparticles with a core size of 13 nm, coating made with polymer B1 and an MNP concentration of 0.04 mg/ml.

C. TEM studies of MNPs

Nanoparticle solutions were dispersed and then dried on copper grids. TEM micrographs were obtained using a JEM 1200 EX II (Jeol Co., Japan) transmission electron microscope operating at 80 kV and recorded on photographic plates, which ensure high resolution. After development, the photographic plates were scanned, and the graphic files were subjected to digital analysis. Images of at least 100 nanoparticles were analysed with ImageJ to determine the size of nanoparticle cores.

D. ATR-FTIR measurements of DMPC/MNP systems

FTIR spectra for all DMPC/MNPs systems were collected on a spectrometer TENSOR 27 (Bruker Optics) and by the use of an ATR attachment with a diamond crystal. Absorption data were collected in the temperature range of 275–313 K with a step size of 2 K. For each measurement, 256 scans at a resolution of 4 cm^{-1} were accumulated. The fitting procedure of absorption peaks was carried out by the use of the second derivative and by using the Opus program package.

III. RESULTS AND DISCUSSION

A. Structural characterisation of magnetic nanoparticles

Exemplary TEM images of the studied magnetic nanoparticles are presented in Figures 1 and 2. Detailed analyses of the images confirmed the expected nanoparticle diameters. Furthermore, the process of nanoparticle modification with different polymers did not cause any morphological changes. The prepared nanoparticles are spherical and have good size and shape monodispersities. No tendency for aggregate formation was observed. High-resolution images confirm the crystalline structure of the magnetic cores of 3 nm nanoparticles (Figure 2).

B. ATR-FTIR of DMPC/MNP systems

Examples of FTIR spectra (and deconvolution) recorded for the investigated DMPC/MNP systems are shown in Figure 3. The FTIR spectra obtained for pure DMPC solution in D_2O exhibit specific vibration characteristics of the chemical groups of phospholipids and the solvent. The spectra recorded for the solutions containing nanoparticles reveal changes in the absorption intensities and a shift of absorption band characteristics of phospholipids (in particular, CH_2 groups). Furthermore, additional peaks appear that are associated with amide bond vibrations at 1650 cm^{-1} (the coating)[43] as well as an additional weak peak (solution 3A1/1) in the vicinity of 1049 cm^{-1}, which can be attributed to P-O-Fe vibrations.[44]

1. Analysis of ν_{as} CH_2 vibrations for DMPC/13B1 and DMPC/10B1 systems

The symmetric vibrations (ν_s) of the CH_2 group are typically analysed for lipid systems; however, the low

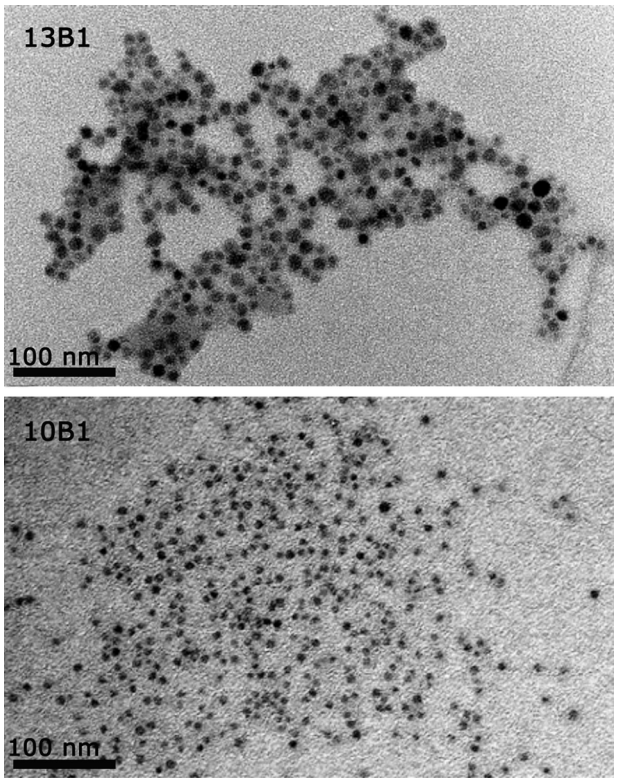

FIG. 1. TEM images of 13B1 nanoparticles with a 13 nm magnetic core (Fe_3O_4) obtained by the thermal decomposition of iron pentacarbonyl and coated with polyacrylic acid and O-(2-aminopropyl)-O′-(2-methoxyethyl)-polypropylene ethylene glycol (PEG1) and 10B1 nanoparticles with a 10-nm magnetic core (Fe_3O_4) obtained by the thermal decomposition of iron pentacarbonyl and coated with polyacrylic acid and O-(2-aminopropyl)-O′-(2-methoxyethyl)polypropylene ethylene glycol (PEG1).

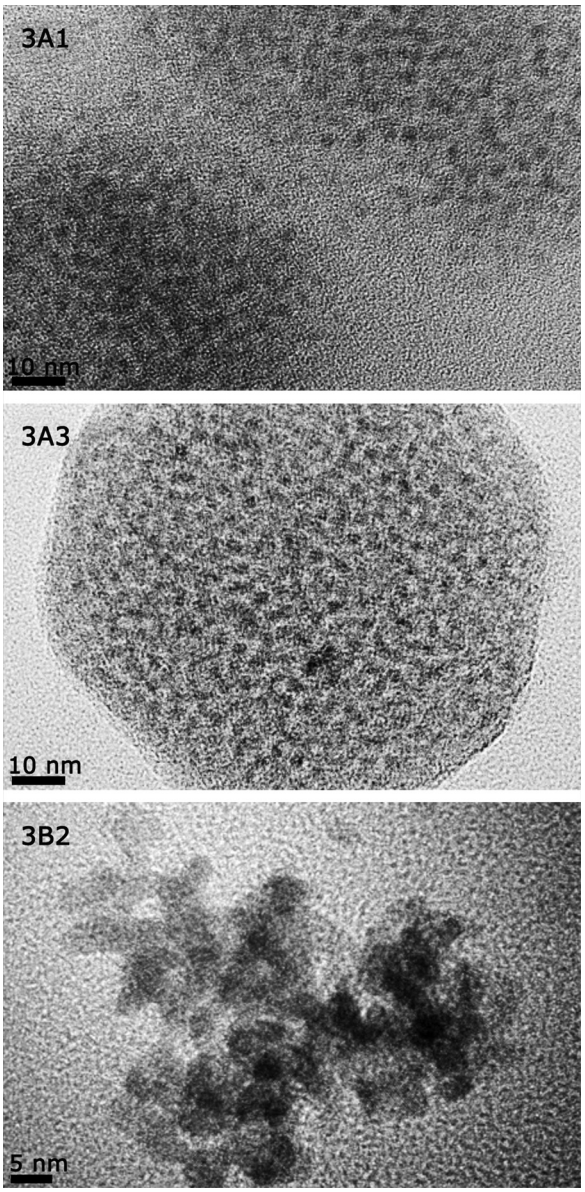

FIG. 2. High-resolution TEM images of 3A1, 3A3, and 3B2.

intensity of these vibrations in our spectra required us to analyse CH_2 asymmetric vibrations (ν_{as}). An example of the deconvolution of absorption curves of the studied systems is presented in Figure 3. In the spectra of a solution of pure DMPC recorded at different temperatures from the range studied, the vibration band ν_{as} (CH_2) is shifted from 2917.5 cm^{-1} at lower temperatures to 2923 cm^{-1} at higher temperatures. A significant change in the wavenumber of approximately 4 cm^{-1} is observed at 295 K (Figure 4), which is close to that of the DMPC main phase transition.[26,37]

The analysis of absorption bands for DMPC systems containing nanoparticles with larger core sizes (13B1 and 10B1) illustrates that there is no shift of the ν_{as} CH_2 absorption band maximum relative to that in a spectrum of pure DMPC solution in the temperature region below the main phase transition (T_m) (Figure 4). For all nanoparticle concentrations, the changes in wavenumbers begin at T_m, associated with the DMPC main phase transition.

For DMPC/13B1 systems at the lowest concentration of MNPs (denoted as 13B1/1), the wavenumber characterising the ν_{as} band maximum at temperatures above T_m rises to 2922 cm^{-1} but then decreases to 2918 cm^{-1} above 309 K (Figure 4(a)). In the spectra of the system with a two-fold concentration of nanoparticles (13B1/2), the absorption peaks are shifted to 2922 cm^{-1}, but a similar decrease in wavenumber (as for the low concentration of MNPs) at higher temperatures is not observed (Figure 4(a)).

The spectra of DMPC/MNP systems with the highest concentration of nanoparticles (13B1/3) exhibit a small increase in wavenumber of approximately 1.5 cm^{-1} above T_m (295 K). Furthermore, a decrease in wavenumber for $T > 300$ K (Figure 4(a)) is clearly observed. The shift of absorption bands observed for systems containing nanoparticles with respect to their positions in the spectrum of the pure DMPC solution is related to a higher ordering of hydrophobic chains of phospholipid molecules (some alkyl chains may remain in the trans conformation), which causes a reduction in membrane fluidity.[28] There is also a significant decrease in the intensity of the absorptive peaks assigned to ν_{as} vibrations of CH_2 groups in the spectra of solutions containing nanoparticles in two extreme concentrations (13B1/1 and 13B1/3) with respect to that in the reference spectrum of the DMPC solution (Figure 4(b)). For the highest concentration (13B1/3), a significant

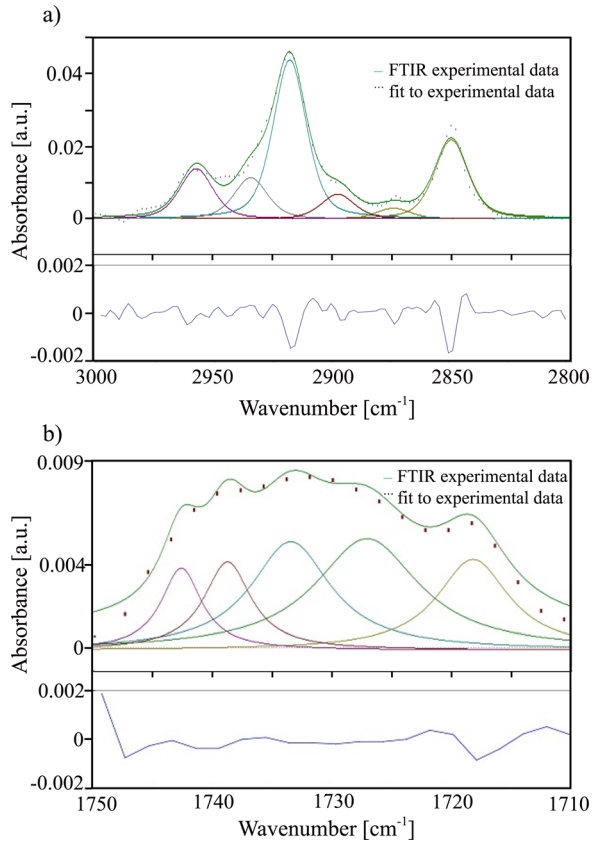

FIG. 3. An example of a deconvoluted FTIR spectrum obtained at the temperature of 283 K in the regions of CH_2 asymmetric (a) and carbonyl (b) stretching modes (top), bottom panel—residuals.

broadening of the absorption peaks assigned to CH_2 groups occurs, and the profile-fitting procedure by the use of the second derivative shows additional components. However, the additional component of asymmetrical CH_3 vibrations at approximately 2928 cm^{-1} also appears for pure DMPC and is occasionally described as overtones.[28]

In DMPC/10B1 systems containing nanoparticles with smaller cores (10 nm), the wavenumbers characterising the absorption band v_{as} of the CH_2 group reaches 2921 cm^{-1} for temperatures below T_m (Figure 4(a)). No tendency toward decreasing the wavenumber characterising the absorption band of the CH_2 group with increasing temperature was observed for these systems. For all DMPC/10B1 systems, the increase in v_{as} is approximately 3 cm^{-1}, whereas the main phase transition in the DMPC lipid matrix begins at T_m, the same as for pure DMPC.

The intensity of ν_{as} vibrations of the CH_2 groups for the two lowest MNP concentrations is comparable to that of the vibrations of the reference DMPC system. The absorption intensity increases for the system with the highest concentration of nanoparticles (DMPC/10B3), and this increase is quite pronounced for $T < T_m$ (Figure 4(b)). However, for the system containing MNPs at a concentration of 0.02 mg/ml, a small decrease in the absorption intensity is observed for $T > T_m$.

For systems containing 10B1 nanoparticles, an additional component of the band appears in the wavenumber region of 2958–2960 cm^{-1}.

2. Analysis of v_{as} CH_2 vibrations for DMPC/3B2, DMPC/3A1, and DMPC/3A3 systems

Analysis of the v_{as} CH_2 bands for all lipid systems containing nanoparticles of small magnetic cores (3B2, 3A1, and 3A3) has shown that this band is not shifted with respect to its position for pure DMPC and systems containing larger MNPs for temperatures $T < T_m$. However, some differences in the stability of the phospholipid structure appear above T_m depending on the type of nanoparticle polymer coating. For DMPC/3B2, the wavenumber corresponding to v_{as} CH_2 is similar for the entire temperature range, although small (~0.5 cm^{-1}) changes in band position appear near T_m for samples with the highest MNP concentration (Figure 5(a)).

In the spectra of the studied systems, a reduction in absorption intensity is noted for the entire range of MNP concentrations (Figure 5(b)) with respect to that in the spectrum of pure DMPC. Some qualitative differences are also observed, such as the broadening of absorption peaks and additional components appearing in the range of 2958–2960 cm^{-1} (Figure 5(a)). For the DMPC/3A1 system with the lowest MNP concentrations, similar changes are observed as for DMPC/3B2, whereas for samples with higher MNP concentrations, significant changes are noted in the IR spectra recorded at temperatures close to T_m. For these systems, the wavenumber corresponding to v_{as} CH_2 vibrations for the highest concentrations of 3B2 nanoparticles (3B2/3) reaches 2924 cm^{-1}, which is similar to that obtained for the reference DMPC system (Figure 5(a)). For all concentrations of 3A1 nanoparticles in the systems based on DMPC, the decrease in intensity of the vibration band is stronger than for the DMPC/3B2 solution (Figure 6). Absorption bands appearing near 1049 cm^{-1} can be assigned to the interactions of PO_2^{2-} groups with magnetite.[36]

The effects of the interaction of nanoparticles 3A3 with DMPC, observed as changes in the FTIR spectra for the systems with the lowest MNP concentrations, are comparable to the changes in position and intensities of the bands in the spectra of 3B2/DMPC. The FTIR spectra of solutions with the highest 3A3 concentrations reveal small changes near T_m, which has also been observed for DMPC/3A1 (Figure 6(a)). For DMPC/3A1, the wavenumber corresponding to CH_2 v_{as} reaches 2919 cm^{-1}. Similarly, as observed for the systems containing 3B2 and 3A3, the intensity of the absorption band (Figure 6(b)) and the shape of the FTIR spectrum are considerably changed.

3. Analysis of C = O vibrations

For analysis of nanoparticle-phospholipid interactions with functional groups on the phospholipid bilayer surface, important information can be obtained from the analysis of $\nu(C=O)$ stretching vibrations in the carbonyl group from the ester group of phospholipids. The carbonyl group from the phospholipid has strong hydrogen interactions with water molecules, leading to the formation of the hydrated form of the phospholipid. The presence of these hydrogen bonds can be detected based on the absorption band of carbonyl group $\nu(C=O)$ at 1728 cm^{-1}. An unhydrated carbonyl group is

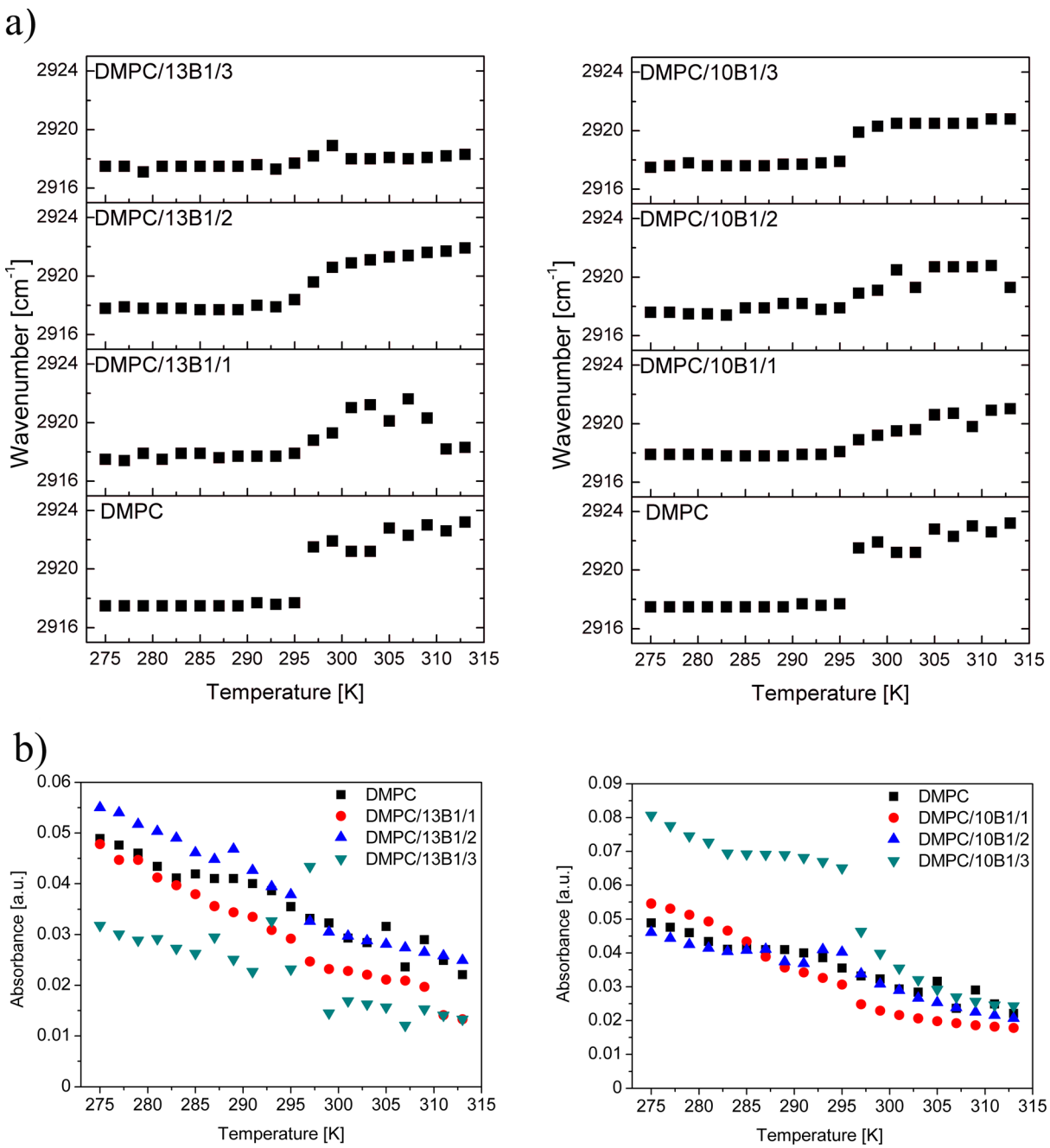

FIG. 4. Wavenumbers characterising the asymmetric CH_2 stretching modes versus temperature for DMPC/13B1 and DMPC/10B1 systems (a). Absorption intensity of asymmetric CH_2 stretching modes versus temperature for DMPC/13B1 and DMPC/10B1 systems (b). The error bars are smaller than the size of the plotted symbols.

characterised by a ν(C = O) stretching band at 1738 cm^{-1}. For all systems studied, the presence of additional components of the absorption band ν(C = O) was observed in the range of 1700–1750 cm^{-1} with magnetic core diameters of 13, 10, and 3 nm.

For the systems containing 13B1 and 10B1, the highest intensity of the components of the ν(C = O) band was observed in the ranges of 1725–1735 cm^{-1} (13B1) and 1738–1745 cm^{-1} (10B1). Comparison of the position of the maximum absorption band of the C=O group in the spectrum of pure DMPC with analogous values for the systems containing the largest concentrations of MNPs, the component of the band for the hydrated carbonyl group is shifted toward higher wavenumbers, whereas that of the band for the unhydrated group is shifted toward lower wavenumbers. In this range, the FTIR spectra have a similar shape as that recorded for the reference DMPC system. A detailed analysis of the stretching vibrations of the carbonyl group has indicated a significant increase in the intensity of the component of the ν(C = O) band corresponding to hydrated carbonyl groups (Figures 7(a) and 7(b)).

The FTIR spectra of the DMPC systems with large nanoparticles (with core diameters of 13 and 10 nm) indicate increased band intensities corresponding to ν_s stretching vibrations of PO_2^{2-} near 1088 cm^{-1}. The error bars are smaller than the size of the plotted symbols.

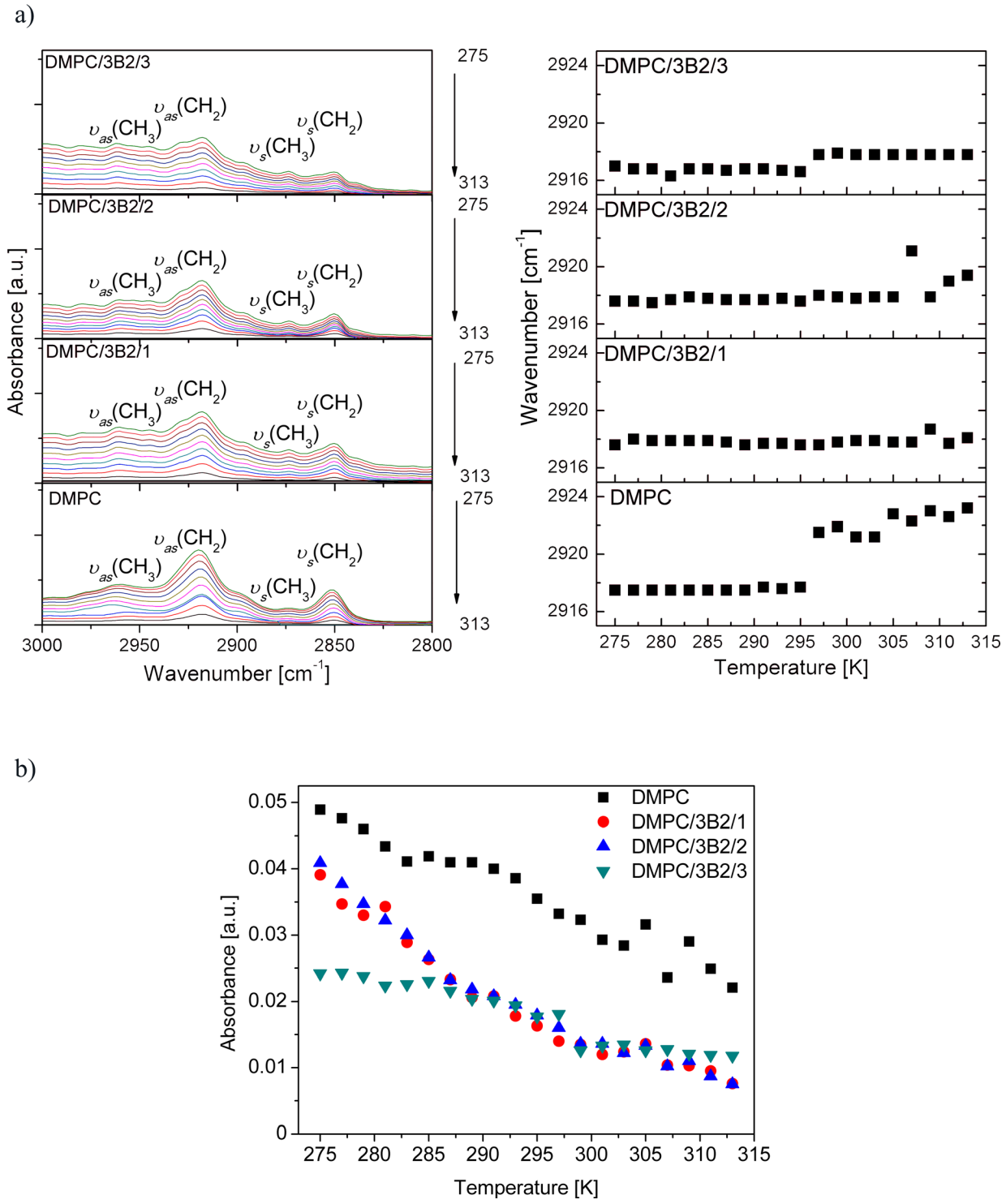

FIG. 5. FTIR spectra recorded for DMPC/3B2 systems (left), wavenumbers characterising asymmetric CH_2 stretching modes versus temperature for DMPC/3B2 (right) (a) and absorption intensity of asymmetric CH_2 stretching modes versus temperature for DMPC/3B2 (b). The error bars are smaller than the size of the plotted symbols.

The FTIR spectra of the systems with the smallest nanoparticles (3B2, 3A1, 3A3) in the range of 1700 –1750 cm^{-1} indicate intensity components comparable with those of the reference DMPC system (Figure 8). After FTIR analysis and careful fitting of the hydrated v(C = O) profile component to FTIR data, the band corresponding to carbonyl group vibrations was also shifted toward higher wavenumbers. For the systems with small nanoparticles (3 nm), this shift was 2–5 cm^{-1} over the entire temperature range. For systems containing larger nanoparticles (13 and 10 nm), the shift of the component corresponding to hydrated carbonyl groups was 5–7 cm^{-1} on average. No increase was observed in the band intensity corresponding to PO_2^{2-} vibrations.

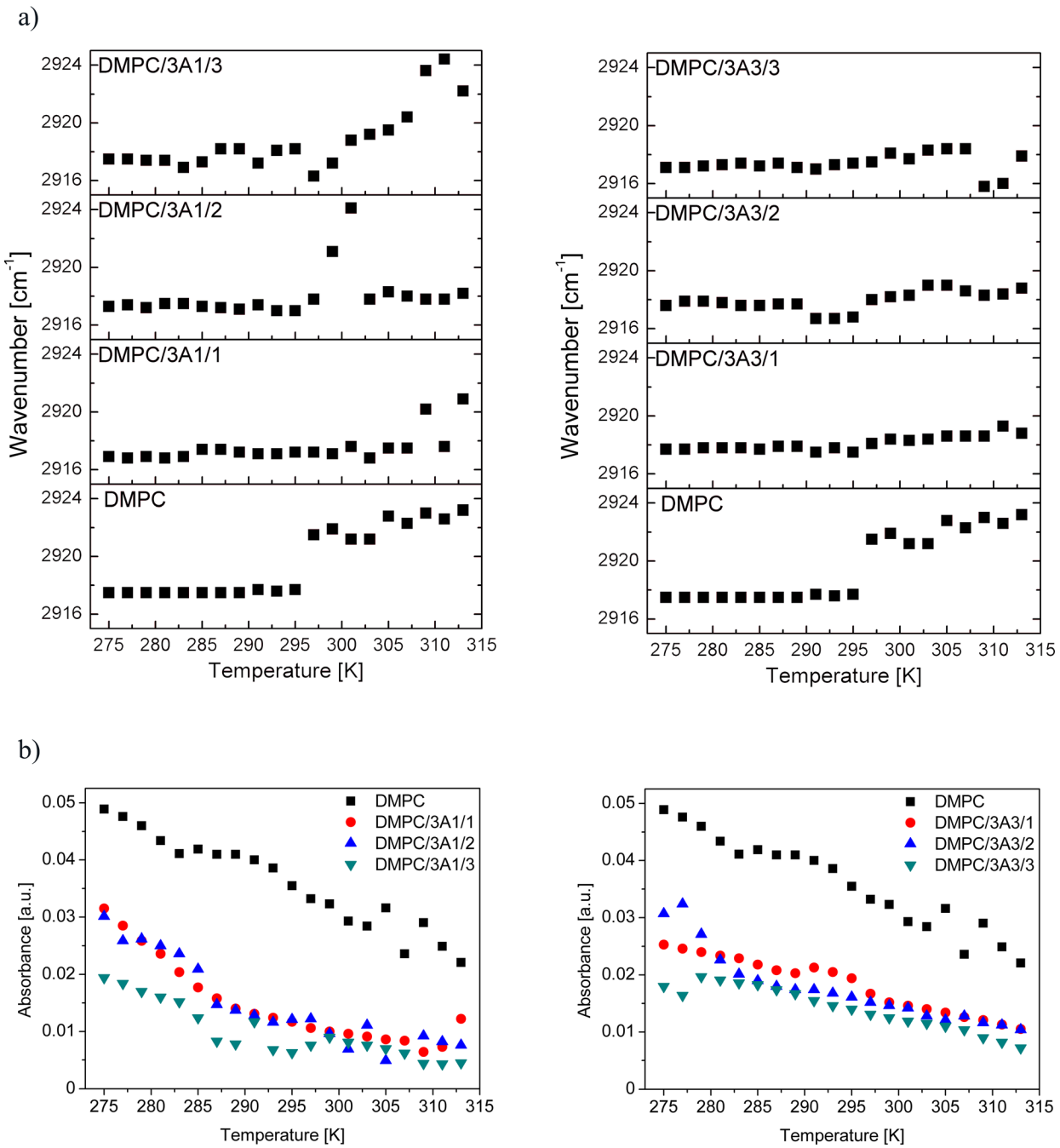

FIG. 6. Wavenumbers characterising asymmetric CH_2 stretching modes versus temperature for DMPC/3A1 and DMPC/3A3 (a). Absorption intensity of asymmetric CH_2 stretching modes versus temperature for DMPC/3A1 and DMPC/3A3 (b). The error bars are smaller than the size of the plotted symbols.

IV. DISCUSSION

The analysis of ν_{as} CH_2 vibrations for DMPC/13B1 and DMPC/10B1 systems shows that nanoparticles with larger core sizes have no impact on the temperature of the main transition (T_m). This observation may suggest that the tested nanoparticles do not interact with the hydrophobic interior of the phospholipid bilayer but rather with its surface, which would confirm the hydrophilic character of the outer shell of the nanoparticles. The lack of shift of the v_{as} CH_2 absorption band maximum in the temperature below T_m (relative to that in a spectrum of pure DMPC solution) can also support the above statement. The appearance of shift of the absorption bands above T_m for the same systems is connected with higher ordering of hydrophobic chains of phospholipid molecules. Assuming that larger hydrophilic nanoparticles do not interact with the interior of the phospholipid bilayer, the formation of a more ordered structure may be connected with surface interactions (the structure could be stabilised by phospholipid surface interactions with nanoparticles).

The significant decrease in the intensity of the absorptive peaks assigned to ν_{as} vibrations of CH_2 groups in the spectra of solutions containing nanoparticles in two extreme concentrations (13B1/1 and 13B1/3) suggests that part of the structure experiences structural degradation, possibly the formation of cavities in the lipid bilayers or even the wrapping (covering process) of nanoparticles by phospholipid

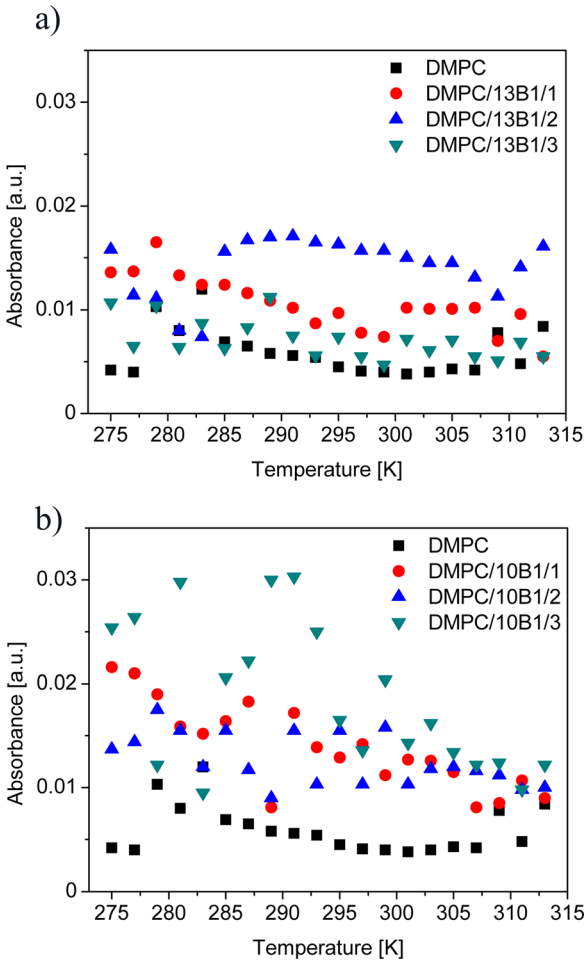

FIG. 7. Absorption intensity of carbonyl group stretching modes versus temperature for DMPC/13B1 (a) and DMPC/10B1 systems (b).

bilayers.[4] Thus, deformations of the lipid bilayers can appear that result in a break in the structure of biomembranes, allowing phospholipid molecules to be extracted from the membrane.[3] An additional component, which occurs at 2928 cm^{-1} in the profile-fitting procedure for the highest concentration of systems with 13 nm nanoparticles (13B1/3) and is occasionally described as overtones for pure DMPC may also suggest that more disordered structures or domains could appear in bilayer systems. The essential aspect in the interpretation of the conformational dynamics and the structure of investigated systems is their comparison with similar systems. Oleson *et al.*[44] reported the possibility of the formation of multiple phospholipid bilayers by the flattening of bilayers that appear after the break of some part of the phospholipid liposomes as a result of interactions with the surface of Al or Si oxides.[44] Multiple supported phospholipid bilayers (SPBs) could form as a result of the attraction and then fusion of flattened dipalmitoylphosphatidylcholine (DPPC) bilayers to the surface of α-Al_2O_3 and α-SiO_2 oxides and their stabilisation across the complex network of interactions (including van der Waals forces, hydrogen bonds, and electrostatic interactions between bilayers).[44,45] Moreover, studies of spherical Al_2O_3 nanoparticles (with diameters of approximately 60 nm) with phosphatidylethanolamine (PE) indicated that liposomal structures could break as a result of

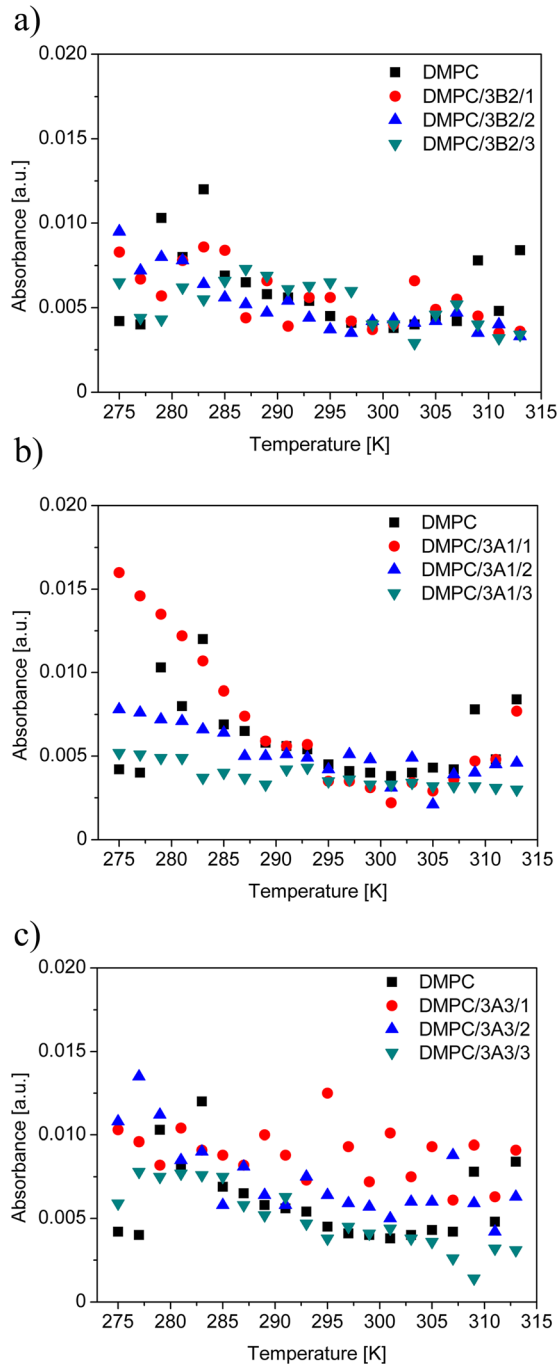

FIG. 8. Absorption intensity of carbonyl group stretching modes versus temperature for DMPC/3B2 (a), DMPC/3A1 (b), and DMPC/3A3 systems (c). The error bars are smaller than the size of the plotted symbols.

interactions between nanoparticles and bilayers, which leads to the creation of similar multilamellar structures around nanoparticles after the fusion process.[46] However, in studies of the influence of spherical SiO_2 nanoparticles on phosphatidylcholine derivatives (dimyristoylphosphatidylcholine (DMPC), dipalmitoylphosphatidylcholine (DPPC), distearoylphosphatidylcholine (DSPC)), the possibility of the formation of SiO_2 nanoparticles covered by a lipid bilayer with attached additional phospholipid molecules was indicated. These molecules were formed as a result of a loosening of the space between hydrophilic heads of phospholipids in the bilayer, which caused the bilayer to stiffen. A tendency of

the interactions between phospholipids and SiO_2 to increase with increasing nanoparticle size was observed and manifested by a shift of the main phase transition toward lower temperatures.[46] Thus, the nanoparticles often lead to the deformation and break of liposomal structures. Based on this effect and the decrease in absorbance, it can be assumed that the investigated nanoparticles (13B1) can cause similar disturbances to the bilayers. One result of such disturbances is systems with ordered domains.

Considering the band intensity and earlier analysis for nanoparticles with a diameter of 13 nm, in the studied systems, the processes of lipid membrane deformation and formation of other structures for systems nanoparticles with a diameter of 10 nm are relatively tame.

Differences in the stability of the phospholipid structure that appear above T_m for all lipid systems containing nanoparticles of small magnetic cores (3B2, 3A1, and 3A3) may suggest that those nanoparticles have greater influence on the phospholipid bilayer. For similar lipid systems containing inorganic nanoparticles, because their size is similar to that of the bilayer, small hydrophilic nanoparticles easily form convex structures, pores, and holes in the membranes, leading to deformation of the lipid bilayer.[1,4,7,23] Reduction in absorption intensity, qualitative differences of absorption peaks, and additional components appearing in the range of 2958–2960 cm^{-1} can be related to the fact that in the same systems and temperature range, different structures may be formed as a result of MNP interactions with phospholipids, including supported bilayers,[4,7,23] that are typically characterised by a lower degree of structural ordering.

The stronger decrease in the intensity of the v_{as} CH_2 $_{bands}$ for all concentrations of 3A1 nanoparticles in the systems based on DMPC provides additional support for the proposed greater influence of small nanoparticles on biomembranes and for the presence of different structural phases induced by phospholipids. The possibility of degradation of the polymer coating of nanoparticles in the endosomal region of the cell and release of nanoparticles from the coating has been reported.[1] Although our studies were performed on a simplified model lipid system, the most likely explanation for this effect is the aggregation of nanoparticles and partial exposition of magnetic cores.

Changes in the shape and intensity of the absorption band observed for the systems 3B2 and 3A3 observations can be explained by the earlier-described influence of small nanoparticles on phospholipid bilayers. Analysis of the full FTIR data for the solutions containing the smallest nanoparticles (core diameter of 3 nm) illustrates that the spectrum of DMPC/3A1 significantly differs in shape from that of the reference DMPC system. The differences are apparent for two concentrations of MNPs (3A1/2 and 3A1/3) and are similar to the effects earlier described for larger nanoparticles described in this work (core diameters of 10 and 13 nm). These effects can be caused by the same polymer coating of (O-(2-aminopropyl)-O′-(2-methoxyethyl)polypropylene ethylene glycol-PEG1) applied in these samples.

Analysis of $\nu(C=O)$ stretching bands connected with nanoparticle-phospholipid interactions with functional groups on the phospholipid bilayer surface revealed the presence of additional components of the absorption band $\nu(C=O)$. It can be a result of the formation of different structural species of lipids (such as bilayers, multilayers, and micelles) in solution as a result of the partial deformation or destruction of liposomes. The earlier conclusions resulting from analysis of CH_2 vibrations also support the proposed appearance of different lipid structures whose carbonyl group vibrations are characterised by different energy parameters (wavenumber and intensity) as a result of the interactions between lipids and MNPs. Based on the results obtained for the earlier-described multilamellar systems,[38] it is reasonable to assume that the components of the band corresponding to carbonyl group vibrations can differ depending on the types of interactions, e.g., interactions of nanoparticles with the bilayer surface or interactions between two subsequent DMPC bilayers. Obtaining an exact definition of the character of interactions between the carbonyl groups from phospholipids and magnetic nanoparticles is difficult. The previously described interactions of inorganic oxides with bilayer surfaces include van der Waals forces, hydration, and electrostatic interactions.[44] For nanoparticles with magnetite Fe_3O_4 cores and a polymer coating based on PEG, there is also a possibility of space penetration between the hydrophilic phospholipid groups by PEG chains. There is also another possibility of interaction between the carbonyl groups of phospholipids and increasing electrostatic interactions (lipid-nanoparticle). Regardless of the character of the interactions of carbonyl groups, the FTIR spectra indicate a shift of the component corresponding to hydrated C=O to higher wavenumbers, which is typically related to the formation of more disordered lipid systems or disordered domains (e.g., bulbs) or even defragmentation of the lipid membrane. The intensity of interactions between nanoparticles and carbonyl groups is also increased as a result of a larger nanoparticle radius, which is indirectly confirmed by the previously described possibility of the insertion of additional phospholipid molecules between the hydrophilic groups (head groups) of DMPC molecules forming a lipid bilayer.

The stronger interactions between small MNPs and carbonyl groups from DMPC observed in this study are not in good agreement with the data reported earlier for lipid/SiO_2 sphere systems.[46] However, we cannot reject the proposed influence of nanoparticle curvature (radius) on the character of their interactions with lipid molecules and/or the possibility of formation of complex lipid structures by the adsorption of additional phospholipid molecules in the space in the DMPC bilayer. We studied nanoparticles with complex chemical composition (in particular, the complex chemical structure of a nanoparticle surface with coatings), and thus, we can assume that in the solutions studied, the coexistence of different lipid structures is possible, and small nanoparticles (their diameter is smaller than the bilayer thickness)[47] may have a toxic effect on biological membranes.[1]

V. CONCLUSIONS

For the studied series of phospholipid systems with magnetic nanoparticles, the influence of nanoparticles on the structure of the model lipid membrane based on DMPC was

quite pronounced for future biomedical applications of these MNP. The strength of this impact was closely related to the size of the magnetic core of the nanoparticles introduced to DMPC. Especially DMPC/13B1 and DMPC/10B1 systems show that nanoparticles with larger core sizes have no impact on the temperature of the main transition of DMPC, which suggests that the tested nanoparticles do not interact with the hydrophobic interior of the phospholipid bilayer but rather with its surface. Additionally, the chemical structure of the polymer coating of the nanoparticles was found to significantly affect the strength of interactions between the nanoparticles and lipid membrane. The effects of MNP interactions with the model lipid membrane observed for nanoparticles with sizes smaller than or similar to the membrane thickness. Interactions between nanoparticles and lipids from the membrane likely lead to the deformation of liposomes, liposome breakage, and the formation of complex ordered structures. The presented characterisation of conformational dynamics in lipid systems containing magnetic nanoparticles is a starting point for a detailed structural investigation of such systems. At this stage of the study, we conclude that the structural changes induced by nanoparticles with small cores (3 nm) in model lipid systems can suggest a nanotoxic character of these nanoparticles. From the perspective of potential medical applications, the influence of nanoparticles on human cells is the most important feature. Further studies should be performed on a wider range of polymer coatings for magnetic nanoparticles to establish the systems and nanoparticle concentrations with the smallest adverse effects on biological membranes.

ACKNOWLEDGMENTS

We would like to thank S. Haracz for nanoparticles preparation. This work was supported by UMO-2012/06/A/ST4/00373 grant from National Science Centre (Poland).

[1]M. Mahmoudi, J. Meng, X. Xue, X. J. Liang, M. Rahman, C. Pfeiffer, R. Hartman, P. R. Gil, W. J. Parak, P. Pino, S. Carregal-Romero, A. G. Kanaras, and S. T. Selvan, Biotechnol. Adv. **32**, 679 (2014).
[2]A. Velikonja, P. B. Santhosh, E. Gongadze, M. Kulkarni, K. Eleršič, Š. Perutkova, V. Kralj-Iglič, N. P. Ulrih, and A. Iglič, Int. J. Mol. Sci. **14**, 15312 (2013).
[3]Y. Roiter, M. Ornatska, A. R. Rammohan, J. Balakrishnan, D. R. Heine, and S. Minko, Nano Lett. **8**, 941 (2008).
[4]V. V. Ginzburg and S. Balijepalli, Nano Lett. **7**, 3716 (2007).
[5]S. Haracz, B. Mróz, J. D. Rybka, and M. Giersig, Cryst. Res. Technol. **50**, 791 (2015).
[6]S. Haracz, M. Hilgendorff, J. D. Rybka, and M. Giersig, Nucl. Instrum. Methods Phys. Res., Sect. B **364**, 120 (2015).
[7]R. Hergt and S. Dutz, J. Magn. Magn. Mater. **311**, 187 (2007).
[8]S. Laurent, S. Dutz, U. O. Häfeli, and M. Mahmoudi, Adv. Colloid Interface Sci. **166**, 8 (2011).
[9]A. Figuerola, R. Coratob, L. Mannaa, and T. Pellegrino, Pharm. Res. **62**, 126 (2010).
[10]C. Hom, J. Lu, M. Liong, H. Luo, Z. Li, J. I. Zink, and F. Tamanoi, Small **6**, 1185 (2010).
[11]S. A. Wahajuddin, Int. J. Nanomed. **2012**, 3445.
[12]J. A. Champion, Y. K. Katare, and S. Mitragotri, J. Controlled Release **121**, 3 (2007).
[13]G. Bao and X. R. Bao, Proc. Natl. Acad. Sci. U.S.A. **102**, 9997 (2005).
[14]S. Zhang, J. Li, G. Lykotrafitis, G. Bao, and S. Suresh, Adv. Mater. **21**, 419 (2009).
[15]H. Gao, W. Shi, and L. B. Freund, Proc. Natl. Acad. Sci. U.S.A. **102**, 9469 (2005).
[16]Y. Pan, S. Neuss, A. Leifert, M. Fischler, F. Wen, U. Simon, G. Schmid, and W. Brandau, Small **3**, 1941 (2007).
[17]R. Vacha, F. J. Martinez-Veracoechea, and D. Frenkel, Nano Lett. **11**, 5391 (2011).
[18]K. Yang and Y. Q. Ma, Nat. Nanotechnol. **5**, 579 (2010).
[19]S. Dasgupta, T. Auth, and G. Gompper, Nano Lett. **14**, 687 (2014).
[20]X. Yi, X. Shi, and H. Gao, Phys. Rev. Lett. **107**, 098101 (2011).
[21]B. D. Chithrani and W. C. Chan, Nano Lett. **7**, 1542 (2007).
[22]M. Desern and W. M. Gelbart, J. Phys. Chem. B **106**, 5543 (2002).
[23]K. A. Smith, D. Jasnow, and A. C. Balazs, J. Chem. Phys. **127**, 84703 (2007).
[24]P. Rivera-Gil, D. Jimenez de Aberasturi, V. Wulf, B. Pelaz, P. del Pino, Y. Zhao, J. M. de la Fuente, I. Ruiz de Larramendi, T. Rojo, X. J. Liang, and W. J. Parak, Acc. Chem. Res. **46**, 743 (2013).
[25]L. Rodriguez-Lorenzo, Z. Krpetic, S. Barbosa, R. A. Alvarez-Puebla, L. M. Liz-Marzán, I. A. Prior, and M. Brust, Integr. Biol. **3**, 922 (2011).
[26]Z. Pietralik, R. Krzysztoń, W. Kida, W. Andrzejewska, and M. Kozak, Int. J. Mol. Sci. **14**, 7642 (2013).
[27]B. Klösgen, *Lipid Bilayers—Structure and Interactions* (Springer-Verlag, Berlin-Heidelberg, 2001).
[28]R. N. A. H. Lewis and R. N. McElhaney, Biochim. Biophys. Acta **1828**, 2347 (2013).
[29]R. N. A. H. Lewis and R. N. McElhaney, Chem. Phys. Lipids **96**, 9 (1998).
[30]R. Koynowa and M. Caffrey, Biochim. Biophys. Acta **1376**, 91 (1998).
[31]C. R. Sanders and J. P. Schwonek, Biochemistry **31**, 8898 (1992).
[32]S. S. Funari, B. Nuscher, G. Rapp, and K. Beyer, Proc. Natl. Acad. Sci. U.S.A. **98**(16), 8938 (2001).
[33]W. Cong, Q. Liu, Q. Liang, Y. Wang, and G. Luo, Biophys. Chem. **143**, 154 (2009).
[34]D. Bach and I. R. Miller, Biochim. Biophys. Acta **1514**, 318 (2001).
[35]U. P. Fringeli, *Encyclopedia of Spectroscopy and Spectrometry* (Academic Press, London, 2000).
[36]M. Cagnasso, V. Boero, M. A. Franchini, and J. Chorover, Colloids Surf., B **76**, 456 (2010).
[37]S. J. Parikh and J. Chorover, Colloids Surf., B **62**, 188 (2008).
[38]S. J. Parikh, F. N. D. Mukome, and X. Zhang, Colloids Surf., B **119**, 38 (2014).
[39]E. J. Elzinga, J. H. Huang, J. Chorover, and R. Kretzschmar, Environ. Sci. Technol. **46**, 12848 (2012).
[40]K. Woo, J. Hong, S. Choi, and H. Weon, Chem. Mater. **16**, 2814 (2004).
[41]N. Insin, Ph.D. thesis, MIT Boston, USA, 2011.
[42]Y. Kim, W. Kim, H. Yoo, and S. K. Shin, Bioconjugate Chem. **21**, 1305 (2010).
[43]S. J. Parikh and L. Chorover, Langmuir **22**, 8492 (2006).
[44]T. A. Oleson, N. Sahai, and J. A. Pedersen, J. Colloid Interface Sci. **352**, 327 (2010).
[45]T. A. Oleson and N. Sahai, J. Colloid Interface Sci. **352**, 316 (2010).
[46]S. Ahmed and S. L. Wunder, Langmuir **25**, 3682 (2009).
[47]J. F. Nagle and S. Tristam-Nagle, Biochim. Biophys. Acta **1469**, 159 (2000).